2018 IEEE/RSJ International Conference on Intelligent Robots and Systems (IROS)
Madrid, Spain, October 1-5, 2018

Aerial Radio-based Telemetry for Tracking Wildlife

Haluk Bayram, Nikolaos Stefas, Volkan Isler

***Abstract*— This paper considers the problem of choosing measurement locations of an aerial robot in an online manner in order to localize an animal with a radio collar. The aerial robot has a commercial, low-cost directional antenna and USB receiver to capture the signal. It uses its own movement to obtain a bearing measurement. The uncertainty in these measurements is assumed to be bounded and represented as wedges. The measurements are then merged by intersecting the wedges. The localization uncertainty is quantified by the area of the resulting intersection. The goal is to reduce the localization uncertainty to a value below a given threshold in minimum time. We present an online strategy to choose measurement locations during execution based on previous readings and analyze its performance with competitive analysis. The time required to localize a target is upper-bounded by the function of measurement noise, desired localization uncertainty and minimum step length. We also validate the strategy in extensive simulations and show its applicability through field experiments over a 5 hectare area using an autonomous aerial robot equipped with a directional antenna.**

I. Introduction

Aerial robots are finding increasing use in challenging problems such as target tracking and localization [1]–[4], wildlife monitoring [5], [6] and package delivery [7]. In this paper, we focus on an environmental monitoring application where the goal is to localize radio-tagged animals using an autonomous Uninhabited Aerial Vehicle (UAV) as illustrated in Figure 1a. Wildlife biologists frequently resort to radio-tagging as a tool for research and management of wildlife, where they attach a radio transmitter to an animal to be tracked and localized. The tags can be put on a collar for large animals such as moose, wolves or bears.

The most basic and common collar is essentially a radio device which broadcasts a Very High Frequency (VHF) radio signal [8]. There are more sophisticated collars equipped with GPS, SMS and/or satellite communication capabilities, but these are usually heavy (which limits their use to only large animals) and expensive (which limits adoption). Therefore we focus on VHF collars, which have been used for 55 years in wildlife tracking. Compared to other types of collars, they are low cost, have reasonable accuracy, and 5-6 times longer life time [9]. Additionally, because of the longevity of VHF collars, the physical interaction with collared animals is minimized, which decreases the possibility of abandonment of a collared animal by its mother or group members. There is a notable disadvantage to VHF, however, manually tracking animals with VHF collars is labor-intensive. In order to estimate the position of the collared animal, various types of ground-based techniques have been used. These include homing in on the animal, triangulation, fixed towers, and vehicle-mounted antennae [10]. The first two techniques are cost-effective but labor-intensive, and the last two require construction and are usually costly. In the homing technique, researchers rely on the fact that signal strength decreases as distance increases. Therefore, they follow the gradient of the signal to locate the animal. This method does not always work because estimating the gradient is difficult due to multi-path effect and interference from the ground or the environment. Often, the directionality of the signal is also used; by rotating the antenna, a coarse bearing measurement is obtained. In the triangulation technique, two or more bearing measurements are merged to localize the animal [11]. Depending on the measurement noise, triangulation performance relies heavily on where the bearing measurements are taken and how far they are from the target. In both the homing and triangulation techniques, walking from one measurement location to another may take long time. During that time, the animal can move, resulting in poor localization performance. UAVs can make the tracking process faster and more accurate, especially when the animal's living area is not easily accessible to humans. Another advantage of using UAVs is the potential for collecting additional data with other types of sensors. For example, once the UAV localizes an animal, it can take a picture or record a video that provides information regarding the interaction between the animal and its habitat. In this paper, we present a system capable of localizing collared animals.

(a) **(b)** **(c)**

Fig. 1: (a) The Online Target Localization Problem: A collared animal is to be localized. The goal is to minimize the time spent in localizing the target in such a way that the localization uncertainty is below a desired level. In the figure, the UAV is moving from s_i to s_{i+1} to take the next bearing measurement. The localization is done by intersecting the bearing measurements. The uncertainty is a function of the measurement locations relative to the (unknown) target location. (b) The quadrotor with an on-board computer, USB receiver and 3-element Yagi antenna. (c) The collar (VHF transmitter operating at 163.739 MHz) used for the radio-tracking of animals.

In VHF-based radio-tracking, the range inference becomes unreliable, since there may be small changes in the characteristics of the received signal due to factors such as the line of sight. However, since bearing is determined by the direction where the signal strength is the strongest, it is not affected by these factors. Hence, our approach is based on bearing measurements. In [12], an EKF-based online algorithm is proposed to localize radio-tagged fish using ambiguous bearing measurements, comparing it with the optimal offline strategy. However, the approach requires a rough initial estimate and noise model, and it is based on ground and surface vehicles. Here, we focus on a UAV-based system. A cooperative search and localization approach is presented in [13]. The localization is done using angle-of-arrival sensor information based

The first author is now with the Department of Electrical & Electronics Engineering, Istanbul Medeniyet University, Istanbul, Turkey. All the work reported in this paper was performed during his postdoctoral studies in the Department of Computer Science & Engineering, University of Minnesota. The other authors are with the Department of Computer Science & Engineering, University of Minnesota, Minneapolis, USA. This work was supported by National Science Foundation Awards #1111638 and #1525045, and MN State LCCMR Program. The authors would like to thank Professor Forest Isbell and Dr. Mark Ditmer for providing the VHF collars, and Cedar Creek Ecosystem Science Reserve for allowing us to do the field experiments at Cedar Creek. {haluk.bayram}@medeniyet.edu.tr, {stefa125, isler}@umn.edu

978-1-5386-8094-0/18/$31.00 ©2018 IEEE

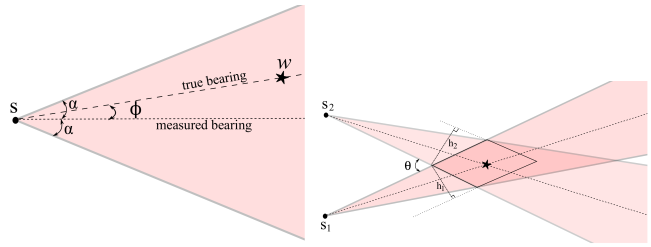

(a) **(b)**

Fig. 2: (a) Sensing model. The target is located at w and known to lie in the measurement wedge. The true bearing is corrupted with unknown but bounded noise α. (b) Approximating the intersection of two measurements as a parallelogram. The target location w is denoted by star.

on existing techniques. The work in [3] proposes a gradient-based approach to localize radio-tagged targets with a low-cost handheld scanner with an omni directional antenna. The performance of the proposed algorithm is compared with the optimal solution through simulations. The work in [14] uses a two-point phased array antenna and custom designed circuitry for signal capturing in order to collect bearing measurements with an aerial robot. The authors present a strategy for choosing measurements so as to improve localization uncertainty to within 50 meters. Our system uses an off-the-shelf antenna and signal receiver, and our bearing strategy provides localization guarantee that is theoretically proven.

Our contributions can be summarized as follows: we present (i) an online algorithm to locate a target using bounded bearing measurements along with a cost analysis of the algorithm, (ii) implementation of the algorithm on a quadrotor to localize a VHF collar, along with the validation of the implementation in field experiments. **Due to space limitations, some of the proofs have been omitted from the paper. They are presented in an accompanying technical report [15]**.

II. Preliminaries

A. Sensing Model & Uncertainty Measure

We consider bearing measurements with bounded noise. The bounded noise model is advantageous over probabilistic models when there is no precise sensor model [16], [17]. In this model, the sensor provides a bearing angle corrupted with a bounded noise α as shown in Figure 2a. The angle difference ϕ between the true bearing and measured bearing is at worst α. The 2D wedge yielded by a measurement is guaranteed to contain the target.

The localization process is performed by intersecting measurements as they are taken. The resulting intersection is considered to be the location uncertainty. The intersection of two bearing measurements can be seen in Figure 2b where the dark shaded area denotes the area in which the target lies. The mathematical representation of the intersection becomes more complicated when the number of measurements increases. We can make a simplification by approximating the intersection as a parallelogram. So, the localization uncertainty U for two measurements taken from locations s_1 and s_2 for a target at location w can be given as the area of this parallelogram [18]:

$$\begin{aligned} U(s_1, s_2, w) = \frac{h_1 h_2}{|\sin\theta|} \quad &\approx \quad \frac{(2d(s_1, w)\tan\alpha)(2d(s_2, w)\tan\alpha)}{|\sin\theta|} \\ &= \quad (2\tan\alpha)^2 \frac{d(s_1, w)d(s_2, w)}{|\sin\theta|} \end{aligned} \tag{1}$$

where the notation $d(a, b)$ denotes the Euclidean distance between points a and b. The term $(2\tan\alpha)^2$ in Equation 1 does not depend on the target-sensor geometry. The rest of the equation is similar to the geometric dilution of precision (GDOP) [19], which is commonly used to measure the uncertainty in estimating the location of a target from two bearing measurements.

B. Problem Statement

Let the true target location be denoted by w. The robot can take bearing measurements of the target location. Each bearing measurement yields a bounded wedge with angular clearance 2α such that the wedge will contain the target. The localization of the target is performed by intersecting the wedges obtained from bearing measurements. Each measurement requires a fixed amount of time τ_m. Locations from which measurements are taken are denoted by s_i for a given measurement i. The full sequence of N measurement locations is $S = \{s_1, \ldots, s_N\}$.

The problem is to determine measurement locations s_i in an online manner so as to localize a target to a desired localization uncertainty $U^\star$ such that the following cost for the localization will be minimized

$$cost(S) = \sum_{i=1}^{N-1} d(s_i, s_{i+1})/v + N\tau_m \tag{2}$$

While the first term in Equation 2 shows the time spent in traveling to each measurement location, the second term corresponds to the total measurement time. For the sake of notational simplicity, the robot is assumed to move at a unit velocity, so the velocity term v will be omitted from the cost function.

III. Online Target Localization

In evaluating the performance of an online algorithm, an optimal offline strategy with knowing the target true location is commonly used. The ratio between the cost of online strategy SOL and the optimal offline strategy OPT is called the **competitive ratio**, which provides an upper bound for how large the cost of the online algorithm can be with respect to the optimal offline strategy. So, we will first derive a lower bound for an offline strategy in order to compute the competitive ratio for the online strategy.

A. Optimal Offline Strategy

We begin by deriving a lower bound on the time required to localize the target when the optimal measurement sequence is used. This sequence is planned in an offline manner with knowledge of the true target location w.

In order to obtain a finite intersection area, at least two measurements need to be taken from two different locations which are not collinear with the target. Therefore, the optimal offline strategy takes at least two measurements.

Proposition 1: Suppose the first measurement is taken from s_1 and the uncertainty in estimating the target's location is desired to be at most $U^\star$. Suppose the second measurement s_2 is taken at (x, y) and the target is located at $(0, 0)$. Using the uncertainty measure in Equation 1, the locus of all such (x, y) is defined by $x^2 + \left(y \pm \frac{C}{2d(s_1,w)}\right)^2 \leq \left(\frac{C}{2d(s_1,w)}\right)^2$ where $C = \frac{U^\star}{(2\tan\alpha)^2}$.

This inequality is the mathematical expression of the **measurement region** for the next measurement s_2, which represents two disks with radius $\frac{C}{2d(s_1,w)} = \frac{U^\star}{2(2\tan\alpha)^2 d(s_1,w)}$ as shown in Figure 3a.

The work in [20] uses a similar derivation for the locus of the next measurement based on the Fisher Information Matrix. However, our uncertainty measure and derivation are solely based on geometry.

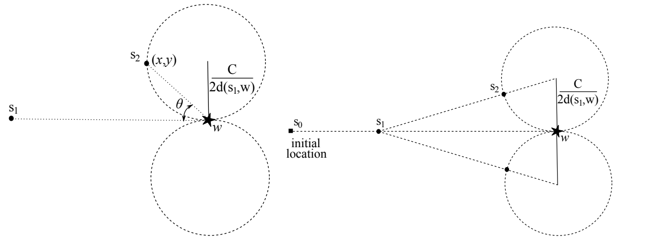

(a) **(b)**

Fig. 3: (a) The measurement region of the second measurement is defined by a disk with radius $\frac{C}{2d(s_1,w)}$ centered at $(0, \pm\frac{C}{2d(s_1,w)})$. The target is known to be at location w. The first measurement is taken from s_1. The second measurement can be taken from the measurement region shown by the dashed circles in order to satisfy the desired uncertainty $U^\star$. (b) Optimal measurement locations. The robot moves from the initial location s_0 to s_1 in order to take its first measurement. Then, the second measurement is taken at the closest point s_2 on the disk to the first measurement location s_1.

In Proposition 1, we assume that the initial location of the robot coincides with the initial measurement location. In the offline case where the target location is known, this choice for the first measurement may lead to a suboptimal solution. In order to rectify this, the robot moves a certain distance towards the target, then takes the first measurement as illustrated in Figure 3b. Then, it moves to the nearest location at the locus where it takes the second measurement. Following this strategy will cost less in terms of distance traveled.

Since the cost in Equation 2 consists of travel time and measurement time, we use the subscripts d for travel (distance) and m for measurement time. For the optimal cost OPT, while OPT_d denotes the cost incurred by OPT for traveling, OPT_m is the time spent in taking measurements.

Theorem 1: Suppose the robot is initially at s_0 and the target is located at w. The cost of the optimal offline solution $OPT = OPT_d + OPT_m$ is lower bounded by $d(s_0, w) - (\sqrt{2}-1)\sqrt{C} + 2\tau_m$.

B. Target On a Line

First, we will consider the case where we would like to localize a target on a known line. We adapt a doubling strategy commonly used for solving online problems such as the lost-cow problem [21].

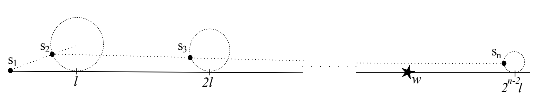

Fig. 4: The measurement locations $\{s_1, \ldots, s_n\}$ computed by the online algorithm applying the doubling strategy in the case where the target is known to be on the line. The dashed circles represent the measurement regions for the corresponding measurements.

In the online algorithm (Algorithm 1) proposed here to localize a target on a known line, the measurement locations are determined in such a way that the possible target locations are hypothesized to be at doubling distances away from the initial location. The next measurement location is determined based on the optimal offline strategy for the current hypothesis. As shown in Figure 4, after the first measurement (Line 4), we can know the direction of the target on the line (Line 5). To determine the second measurement location (Line 11), the target is assumed to be at the location l away from the initial location. Based on this assumption, the measurement region of the second measurement is calculated using the inequality in Proposition 1. The next measurement location will be the point in the measurement region that is closest to the previous measurement location. After each measurement, if the target is not localized (Line 8), its possible location is determined such that it will be further away from the previous location in a doubling manner (Line 19). In some cases, the robot may overshoot the target without localizing it; the next measurement will account for this by indicating a reverse direction (Line 14). After that, instead of applying the doubling strategy, the next possible target location is determined using the halving strategy (Line 21).

Algorithm 1 `Localize-Target-on-Line`

1: $i \leftarrow 1$ {Initialize the measurement index}
2: $m \leftarrow 1$
3: $strategy \leftarrow$ DOUBLING
4: Take the initial bearing measurement s_1 on the line
5: Determine the direction of the target dir {1 for right, -1 for left}
6: Initialize the distance l
7: $w' \leftarrow dir \times l$ {The target is assumed to be w' away from the initial measurement location on the dir side}
8: **while** $U > U^\star$ and $m \neq 0$ **do**
9: {Keep repeating as long as the uncertainty U is higher than the desired uncertainty $U^\star$}
10: $i \leftarrow i + 1$
11: Determine the next measurement location s_i based on the assumption that the target is w' away from s_{i-1}
12: Take a bearing measurement at s_i
13: **if** $i > 2$ and the returning condition is met **then**
14: $dir \leftarrow -1 \times dir$ {Reverse the motion direction}
15: $strategy \leftarrow$ HALVING
16: $m \leftarrow i$
17: **end if**
18: **if** $strategy$ is DOUBLING **then**
19: $l \leftarrow 2l$ {Apply the doubling strategy}
20: **else**
21: $l \leftarrow l/2$ {Apply the halving strategy}
22: $m \leftarrow m - 1$
23: **end if**
24: $w' \leftarrow w' + dir \times l$ {The target is assumed to be w' away from the previous location on the dir side}
25: Compute the localization uncertainty U by intersecting the measurements
26: **end while**

Theorem 2: Suppose the target is located on a line. Given the measurement noise α, the desired localization uncertainty $U^\star$ and the minimum step length l, the online algorithm described in Algorithm 1 has a competitive ratio of $\max\left(\frac{\frac{3\pi}{2}L}{L-\left(\sqrt{2}-1\right)\sqrt{C}}, \log_2\left(\frac{2L}{l}+2\right)\right)$ where L is the distance between the target and the initial location of the robot and $C = \frac{U^\star}{(2\tan\alpha)^2}$.
A sample scenario from the simulations conducted using Algorithm 1 is shown in Figure 5. After the 6th measurement, the robot realizes that it overshot the target and begins applying the halving strategy. After taking the 9th measurement, the robot locates the target within the desired uncertainty.

C. Target Localization on the Plane

Based on the strategy in the online algorithm proposed for the case where the target is on a line, we will extend the algorithm to the problem in which the target can lie anywhere in a 2D environment.

In this case, we do not have any prior knowledge about the target location, unlike the case where the target is on a line. But if the

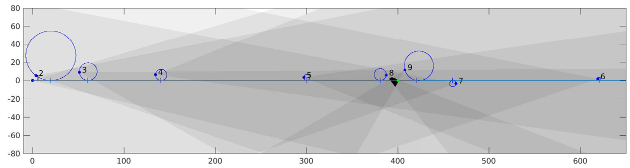

Fig. 5: A sample from the simulations where the target is known to be on the line, but its location on this line is not known. The bearing noise α is set to $\pi/12$. The ticks on the line show the assumed target locations. The disks represent the measurement region for an assumed target location. The thick dots show the measurement locations. After 9 measurements, the target is localized. The final localization uncertainty is black in color.

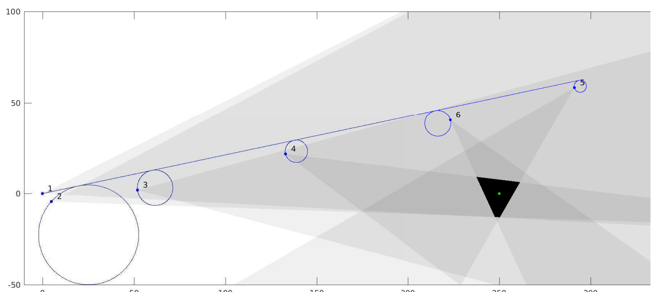

Fig. 6: A sample from the simulations where the target can be anywhere on a plane. The bearing noise α is set to $\pi/12$. The target is close enough to the bisector of the first measurement in order to localize it up to the desired uncertainty by executing Algorithm 1.

bearing noise α is small enough, we can make the assumption that the target lies on the bisector of the first measurement. Therefore, the strategy in Algorithm 1 can be applied to the target in 2D under this assumption. The validity of the assumption highly depends on how far the target is from the initial location and the desired localization uncertainty, which in turn will affect the localization performance. The larger the measurement noise α is, the more the localization performance deteriorates.

Figure 6 shows a sample from the simulations where the target can be anywhere on a plane. The target can be localized due to its proximity to the bisector. However, if the distance from the bisector grows, Algorithm 1 cannot localize the target.

We turn this insight into a new strategy by detecting this situation and resetting the strategy, which is described in Algorithm 2. At

Algorithm 2 `Localize-Target-on-Plane`

1: **while** Target is not localized **do**
2:     Call `Localize-Target-on-Line` (Algorithm 1)
3: **end while**

the onset of the mission, after taking a bearing measurement, the algorithm applies the doubling strategy by increasing i by one until the returning step $i = k$ is detected. Then, the halving strategy is applied by decreasing i by 1 until $i = 0$. The procedure described so far is what Algorithm 1 proposes. At this point, there are two possibilities: (i) the target is localized, either because our assumption (that the target is on the line defined by the bisector of the first measurement) holds or because the desired localization uncertainty $U^\star$ is large enough to localize the target using the line strategy, (ii) the target is not localized because it is far away from the line or the desired uncertainty $U^\star$ is small. In the latter case, `Localize-Target-on-Plane` (Algorithm 2, Line 2) calls `Localize-Target-on-Line` (Algorithm 1) again by assuming the target lies on the line defined by the bisector of the measurement taken when i is decreased to 0. The restarting process

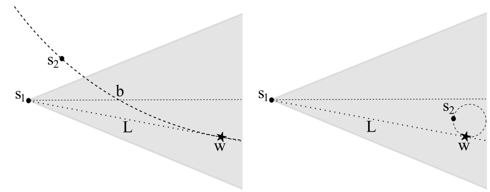

(a) Case-I **(b)** Case-II

Fig. 7: For both cases, the offline optimal solution takes the second measurement from s_2 on the measurement region. (a) In Case-I, the measurement region for the first measurement intersects the bisector of the first measurement. After the first measurement, the online algorithm determines the next measurement locations based on the assumption that the target is on the bisector. Whenever a measurement is taken within the measurement region, the target is guaranteed to be localized. (b) In Case-II, since the measurement region generated by considering the first measurement location s_1 and the target location w does not intersect the bisector of the first measurement, the online strategy first needs to realize that the target cannot be localized under the assumption that it is on the line, hence the online strategy should determine where it leaves the line.

is repeated until the target is localized.

The analysis of `Localize-Target-on-Plane` can be divided into two cases based on the size of the measurement region generated for the offline optimal solution and whether the measurement region intersects the bisector of the first measurement:

- Case-I: The measurement region intersects the bisector and is large enough such that the bisector lies in the region. Therefore, there exists a measurement taken within this measurement region under the assumption that the target is on the bisector. Executing Algorithm 1 once will be sufficient to localize the target as in Figure 6.
- Case-II: Either the measurement region does not intersect the bisector, or the measurement region intersects the bisector but does not contain any measurement location generated assuming the target is on the bisector. This case requires restarting of Algorithm 1 after it fails to localize the target under the assumption that the target is on the current bisector. A sample simulation for Case-II can be seen in Figure 8.

Case-I is depicted in Figure 7a. Here the offline optimal solution moves to the location s_2 on the measurement region with radius $\frac{C}{2L}$ by traveling $d(s_1, s_2) = L - (\sqrt{2}-1)\sqrt{C}$. The online strategy needs to move beyond location b, which is the intersection of the measurement region's boundary and the bisector. The distance $d(s_1, b)$ can be at most L. So the last measurement can be taken from a location which is at worst $2L$ away from s_1. While the offline optimal solution requires only two measurements, the online strategy takes at most $n = \log_2(\frac{L}{l}) + 1 = \log_2(\frac{2L}{l})$ measurements. Hence, the costs of the optimal solution and the online strategy are as follows:

$$\begin{aligned} OPT &= OPT_d + OPT_m \geq L - (\sqrt{2}-1)\sqrt{C} + 2\tau_m \\ SOL &= SOL_d + SOL_m \leq 2L + \log_2(2L/l)\tau_m \\ &\leq \frac{2L}{L - (\sqrt{2}-1)\sqrt{C}} OPT_d + \frac{\log_2(2L/l)}{2} OPT_m \\ &\leq \max\left(\frac{2L}{L - (\sqrt{2}-1)\sqrt{C}}, \log_2(\sqrt{\frac{2L}{l}})\right) OPT \end{aligned} \quad (3)$$

Case-II is depicted in Figure 7b. As in Case-I, the offline optimal solution moves to the location s_2 on the measurement region with the radius $\frac{C}{2L}$ by traveling $d(s_1, s_2) = L - (\sqrt{2}-1)\sqrt{C}$. Since the target w is not on the line or close enough to the line, the online

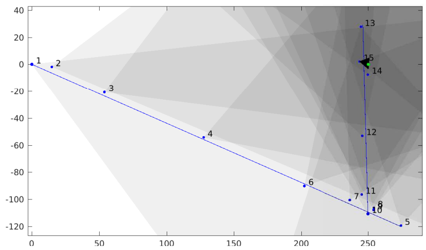

Fig. 8: A sample from the simulations for Case-II. The bearing noise α is set to $\pi/6$. The thick dots show the measurement locations. After the 15th measurement, the target is localized. The final localization uncertainty is shaded by black color.

algorithm cannot localize it just by moving on the line. After the returning location where the angle between the current bisector and the bearing is greater than $\pi/2$, the online algorithm starts applying the halving strategy at the location s_κ until the index i decreases from κ to 0.

Lemma 1: Assuming the target is on the line defined by the bisector of the first measurement, `Localize-Target-on-Line` starts applying the halving strategy after taking, at worst, κth measurement where $\kappa = \left\lceil \log_2 \left(\frac{2L}{l} \sec\alpha + 2 \right) \right\rceil$.

The robot leaves the line when the step index i is decreased to 0. Now it is assumed that the target is on the bisector of the measurement taken at this leaving location. The number of repetitions of this process can be upper-bounded by forcing the robot to enter the measurement region with radius $\frac{C}{2L}$ defined by the first measurement (using Proposition 1).

Lemma 2: To localize a target on 2D, `Localize-Target-on-Line` is recalled at most γ times where $\gamma = \frac{\log_2 \left(\frac{C}{2L^2} \right)}{\log_2 \left(\tan\alpha \right)}$.

Theorem 3: Given the measurement noise α, desired localization uncertainty $U^\star$ and minimum step length l, `Localize-Target-on-Plane` has a competitive ratio of $\max \left(\frac{2\gamma L \sec\alpha}{L - (\sqrt{2}-1)\sqrt{C}}, \kappa\gamma \right)$ where L is the distance between the target and the initial location of the robot and $C = \frac{U^\star}{(2\tan\alpha)^2}$.

IV. Implementation and Experiments

We now evaluate Theorem 3 through extensive simulations and show the applicability of Algorithm 2 on an aerial robot. We verify the bound on the performance of the localization approach presented in the paper and implement the algorithm in locating radio-tags to facilitate wildlife tracking studies.

A. Simulations

`Localize-Target-on-Plane` is repeated 1000 times for random initial positions of the robot and random positions of the target with varying distances between them $L = \{150, 300, 600, 1200\}$ meters and also for uniformly distributed bearing noise with varying maximum corruption $\alpha = \{\pi/12, \pi/6\}$ radians. For all the simulations, the desired localization uncertainty $U^\star$ was set to 315 m^2, which corresponds to the area of a disk with radius 10 meters. The minimum step length l is set to the radius of the corresponding disk of the desired localization uncertainty. The robot's speed is set to 15 m/sec in order to make it consistent with the real system. Each bearing measurement takes 2 minutes.

A sample simulation result for L=300 meters and α=$\pi/12$ radians can be seen in Figure 6. In this scenario, the robot starts taking the first measurement from the initial location. Using the proposed strategy, it locates the target with six measurements up to the desired localization uncertainty.

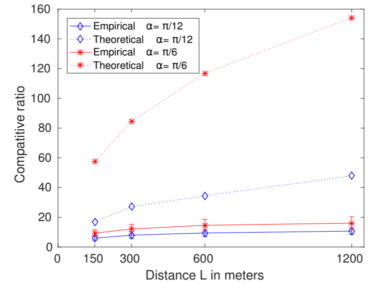

Fig. 9: Empirical and theoretical competitive ratio.

We report the ratio of the localization time SOL and the lower bound of the optimal solution OPT (Theorem 1) in Figure 9. The localization time SOL is calculated using Equation 2. All of the data points and their error bars in the figure show the mean value and standard deviation of 1000 simulations conducted under the corresponding setting. With this ratio (a.k.a competitive ratio) obtained from the simulations, we can see how tight of a bound the competitive ratio in Theorem 3 is. As shown in Figure 9, the theoretical bound is much more vulnerable to the change in the distance L, compared to the change in the bearing noise α. On the other hand, the empirical competitive ratio is more robust to the change in L and α than the theoretical bound. The empirical ratio is less than 16.5, far below the theoretical bound.

B. Field Experiments

We begin with the description of the hardware and software infrastructure of the system. Then we present the field experiments.

1) System Description: Our system consists of an aerial robot with an on-board computer and sensors (GPS, IMU, compass), and radio-tracking components (signal receiver, directional antenna and a radio transmitter collar attached to the animal). The aerial robot used in this work is a quadrotor DJI Matrice 100 (Figure 1b). It has a takeoff weight of 3.4 kg, flies for approximately 25 minutes with two batteries, and travels at speeds of up to 17 m/sec with a payload of 1 kg. The onboard processor is an NVIDIA Jetson TX1 computer with an Ubuntu 16.04 Linux operating system and ROS-based framework. The ROS (Robot Operating System) middleware allows for integration of our various components into the system. All processing is performed online with the on-board computer. A WiFi module enables communication with a ground station laptop computer, which is used only for observing the status of the UAV. Autonomous GPS waypoint navigation with ROS-based integration is provided by the manufacturer with a hovering accuracy of 2.5 meters. The developed online algorithm was implemented as a ROS node on this framework.

As shown in Figure 1b, the UAV has a 3-element Yagi antenna mounted underneath. The antenna is connected to an inexpensive RTL-SDR (Software Defined Radio) USB receiver, which is tuned to the collar's frequency [22]. The signal captured by the USB receiver is read in IQ data format through `rtl_sdr` software[1], which is an IQ recorder for RTL2832 based DVB-T receivers. (Please refer to the accompanying video for how to take bearing measurements)

The target is tagged with a collar, which is a Telonics MOD-500 VHF radio transmitter operating at the pre-set frequency 163.739 MHz (Figure 1c). The collar transmits 80 pulses with a width of

[1] `rtl_sdr` software is available at `http://osmocom.org/projects/sdr/wiki/rtl-sdr`

Fig. 10: A sample field experiment at Cedar Creek Ecosystem Science Reserve, MN.

15 msec in active mode and 40 pulses per minute in inactive mode, respectively.

2) Field Trials: `Localize-Target-on-Plane` (Algorithm 2) was implemented on the quadrotor UAV (Figure 1b). The localization strategy and analysis of bearing measurements were coded as a ROS node in Python so that the UAV can perform its task autonomously. All of the processing is done on the UAV. The ground station is used only for observing the current state of the UAV.

The system was tested at Cedar Creek Ecosystem Science Reserve where the wildlife biologists plan to tag wolves with VHF collars. The collar was deployed at a location 150 meters away from the initial location of the UAV. The flight altitude was about 30 meters. Based on the bearing measurement analysis, the bearing noise α was set to $\pi/6$ radians. The desired localization uncertainty $U^{\star}$ was set to 315 m^2, which corresponds to the area of a disk with radius 10 meters. The robot runs its localization task until the localization uncertainty is below $U^{\star}$. The minimum step length l was chosen as the radius (10 meters) of the corresponding disk of the desired localization uncertainty.

A sample field experiment is shown in Figure 10. The location of the collar is marked by "T". Each measurement is shown as a gray wedge. The UAV starts at the first measurement location M-1. Until the fourth measurement, the UAV applies the doubling strategy. After that, the halving strategy is applied. After the fifth measurement, M-5, the target is localized to the desired localization uncertainty. The whole experiment took 13 minutes, which is a duration that the UAV can fly for with one battery. In the field experiments, the collar was in active mode.

V. Conclusion

In this work, we proposed an online strategy to choose measurement locations during execution so as to localize VHF radio collared animals using an aerial robot. We showed the performance of the online strategy with competitive analysis. We also demonstrated the strategy's applicability in field experiments using an autonomous aerial robot equipped with a directional antenna. In the next stage, the flight time will be improved by optimizing the measurement time and the analysis of the captured signal. We would also like to revise the system design and reduce the payload to be able to use two batteries. To achieve long-term autonomy, in case of insufficient power, the UAV will be made to be able to go to a home position in order to replace (or even recharge) the battery, and then resume its localization task. Our future work will also focus on extending the strategy to use multiple aerial robots. One of the main challenges in the multirobot extension is to maintain communication to exchange their measurement history.

References

[1] F. Korner, R. Speck, A. H. Göktogan, and S. Sukkarieh, "Autonomous airborne wildlife tracking using radio signal strength," in *IEEE/RSJ Int. Conf. on Intelligent Robots and Systems*, 2010, pp. 107–112.

[2] P. Tokekar, D. Bhadauria, A. Studenski, and V. Isler, "A robotic system for monitoring carp in Minnesota lakes," *Journal of Field Robotics*, vol. 27, no. 6, pp. 779–789, 2010.

[3] H. Bayram, K. Doddapaneni, N. Stefas, and V. Isler, "Active localization of VHF collared animals with aerial robots," in *2016 IEEE Int. Conf. on Automation Science and Engineering*, 2016, pp. 934–939.

[4] H. Bayram, N. Stefas, K. S. Engin, and V. Isler, "Tracking wildlife with multiple UAVs: System design, safety and field experiments," in *Int. Symp. on Multi-Robot and Multi-Agent Systems*, 2017, pp. 97–103.

[5] J. C. Hodgson, S. M. Baylis, R. Mott, A. Herrod, and R. H. Clarke, "Precision wildlife monitoring using unmanned aerial vehicles," *Scientific Reports - Nature*, vol. 6, no. 22574, 2016.

[6] M. Dunbabin and L. Marques, "Robots for environmental monitoring: Significant advancements and applications," *IEEE Robotics & Automation Magazine*, vol. 19, no. 1, pp. 24–39, 2012.

[7] M. Heutger and M. Kückelhaus, "Unmanned aerial vehicle in logistics - a DHL perspective on implications and use cases for the logistics industry," *DHL Customer Solutions & Innovation*, 2014.

[8] A. R. Klegarth, "Home range," in *The International Encyclopedia of Primatology*. John Wiley & Sons, Inc., 2016.

[9] L. D. Mech and S. M. Barber, "A critique of wildlife radio-tracking and its use in national parks - a report to the U.S. National Park Service," Tech. Rep., 2002.

[10] L. D. Mech, *Handbook of Animal Radio-Tracking*. University of Minnesota Press, 1983.

[11] R. A. G. Gary C. White, *Analysis of Wildlife Radio-Tracking Data*. Academic Press, 1990.

[12] J. Vander Hook, P. Tokekar, and V. Isler, "Cautious greedy strategy for bearing-only active localization: Analysis and field experiments," *Journal of Field Robotics*, vol. 31, no. 2, pp. 296–318, 2014.

[13] D. J. Pack, P. DeLima, G. J. Toussaint, and G. York, "Cooperative Control of UAVs for Localization of Intermittently Emitting Mobile Targets," *IEEE Transactions on Systems, Man, and Cybernetics, Part B (Cybernetics)*, vol. 39, no. 4, pp. 959–970, 2009.

[14] O. Cliff, R. Fitch, S. Sukkarieh, D. Saunders, and R. Heinsohn, "Online Localization of Radio-Tagged Wildlife with an Autonomous Aerial Robot System," in *Proceedings of Robotics: Science and Systems*, Rome, Italy, July 2015.

[15] H. Bayram, N. Stefas, and V. Isler, "Aerial radio-based telemetry for tracking wildlife," Department of Computer Science and Engineering, Univeristy of Minnesota, Tech. Rep. 17-004, 2017. [Online]. Available: https://www.cs.umn.edu/research/technical_reports/view/17-004

[16] V. Isler and R. Bajcsy, "The Sensor Selection Problem for Bounded Uncertainty Sensing Models," *IEEE Transactions on Automation Science and Engineering*, vol. 3, no. 4, pp. 372–381, 2006.

[17] P. Tokekar and V. Isler, "Sensor placement and selection for bearing sensors with bounded uncertainty," in *IEEE Int. Conf. on Robotics and Automation*, 2013, pp. 2515–2520.

[18] R. J. Bamberger, J. G. Moore, R. P. Goonasekeram, and D. H. Scheidt, "Autonomous Geo location of RF Emitters Using Small, Unmanned Platforms," *Johns Hopkins APL Technical Digest*, vol. 32, no. 3, pp. 636–646, 2013.

[19] A. Kelly, "Precision dilution in triangulation based mobile robot position estimation," in *Proceedings of the Int. Conf. on Intelligent Autonomous Systems*, Amsterdam, 2003.

[20] J. V. Hook, P. Tokekar, and V. Isler, "Algorithms for cooperative active localization of static targets with mobile bearing sensors under communication constraints," *IEEE Transactions on Robotics*, vol. 31, no. 4, pp. 864–876, 2015.

[21] R. A. Baieza-Yates, J. C. Culberson, and G. J. E. Rawlins, "Searching with uncertainty," Indiana Univeristy, Tech. Rep. 239, 1988.

[22] K. VonEhr, S. Hilaski, B. E. Dunne, and J. Ward, "Software Defined Radio for direction-finding in UAV wildlife tracking," in *IEEE Int. Conf. on Electro Information Technology*, 2016, pp. 464–469.